Mendeleev Commun., 2025, **35**, 211–213

Catalytic conversion of fatty acid methyl esters over bimetallic Pt–Cu catalyst based on copper phyllosilicate

Victoria S. Zhuravleva,[a,b] Anastasiya A. Shesterkina,*[a] Anna A. Strekalova,[b] Ekaterina M. Smirnova,[c] Kseniia V. Vikanova,[a] Sergey F. Dunaev[a] and Alexander L. Kustov[a]

[a] *Department of Chemistry, M. V. Lomonosov Moscow State University, 119991 Moscow, Russian Federation. E-mail: anastasiia.strelkova@mail.ru*

[b] *N. D. Zelinsky Institute of Organic Chemistry, Russian Academy of Sciences, 119991 Moscow, Russian Federation*

[c] *National University of Oil and Gas ‘Gubkin University’, 117917 Moscow, Russian Federation*

DOI: 10.71267/mencom.7591

The catalytic properties of bimetallic Pt–Cu catalyst based on SiO_2 support were explored in the selective hydrogenation of fatty acid methyl esters. The synthesized catalysts were investigated by XRD, TEM-EDX and TPR-H_2 methods. The best catalytic properties were achieved over 1Pt/10Cu-PhySi catalyst at temperature 240 °C and H_2 pressure of 2.5 MPa.

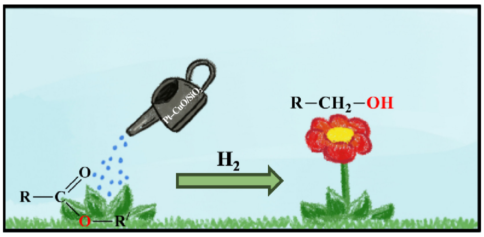

Keywords: bimetallic Pt–Cu catalyst, copper catalyst, copper phyllosilicate, ester hydrogenation, FAMEs, fatty alcohols.

The hydrogenation of fatty acids and esters derived from bio-based feedstocks, which are triglycerides contained in natural oils and fats, is an important process employed to obtain fatty alcohols and other chemicals.[1–4] Higher alcohols, particularly long-chain alcohols such as butanol, hexanol, oleyl alcohol and octadecanol, are industrially important components for the production of surfactants and softeners, as well as for the production of flavourings,[5,6] pharmaceuticals,[7] solvents,[8] emulsifiers, lubricants and organic synthesis intermediates.[9,10]

There are several ways to produce fatty alcohols. The traditional production of alcohols implies the selective hydrogenation of esters using inorganic hydrides (sodium and lithium borohydrides) as hydrogen donors. This approach allows obtaining the desired alcohols under mild conditions with high selectivity, but the disadvantages of this method are the toxicity and explosiveness of the compounds along with the large quantity of difficult-to-separate wastes generated during the reaction.[11] Besides, higher alcohols are synthesized by hydrogenation of esters produced by transesterification reaction between fats (vegetable oil) and methanol (methanolysis) or by hydrogenation of fatty acids obtained by the hydrolysis of fats (vegetable oil).[12,13]

Copper-based catalysts are the most efficient in the hydrogenation of esters inasmuch as Cu is active for C=O bond hydrogenation and inactive for C–C bond hydrogenolysis.[14–16] Among a large variety of copper-based catalysts, catalytic systems with phyllosilicate structure are of special interest due to high dispersion of Cu nanoparticles, large specific surface area of the support and the prospect of using these systems in high-temperature reactions.[17,18] Di *et al.*[19] reported the effect of NH_4^+ and Zn^{2+} on the structure of Cu/SiO_2 catalyst with phyllosilicate phase in the hydrogenation of ethyl acetate to ethanol. It was found that the addition of NH_4^+ and Zn^{2+} ions resulted in the formation of small copper nanoparticles which favored to an increase of catalysts activity and yielded high conversion of ethyl acetate (> 97%) and high selectivity of EtOH (> 99%) in the temperature range 230–250 °C, H_2 pressure of 3.0 MPa and at H_2/ethyl acetate molar ratio equal to 29. As it was shown in our previous work,[20] Cu phyllosilicate-based catalysts have proven to be an efficient and promising catalytic systems for the selective hydrogenation of dimethyl oxalate to ethylene glycol. Here, we investigated catalytic properties of Cu phyllosilicate in the selective hydrogenation of fatty acid methyl esters (FAMEs) and the effect of the second metal (Pt) addition on the catalytic activity in this process.

The synthesis method of the bimetallic copper phyllosilicate-based catalysts is described.[†] The catalytic properties of all the

---

[†] The 10% Cu/SiO_2 catalysts with the phyllosilicate structure (10Cu-PhySi) were prepared by deposition–precipitation of $Cu(NO_3)_2$ on the SiO_2 support using thermal hydrolysis of urea (DPU-method). For comparison, a 10% Cu/SiO_2 catalyst was synthesized by wetness impregnation method (10CuO/SiO_2). A detailed synthesis of monometallic copper samples was described in our earlier work.[17] Supported bimetallic catalyst with 1 wt% of Pt was synthesized by the incipient wetness impregnation of the 10Cu-PhySi sample with an aqueous solution of metal precursor H_2PtCl_6 (Aurat). Then impregnated samples were dried at 90 °C for 12 h and calcined in air at 300 °C for 3 h. The phase composition of the samples was detected by X-ray diffraction (XRD) method using an ARL X’TRA diffractometer (Thermo Fisher Scientific). The morphological properties of the catalysts were investigated by TEM method using a JEOL JEM-2100 transmission electron microscope. The character of the reduction of the synthesized catalysts was examined by temperature-programmed hydrogen reduction (TPR-H_2) method using an AutoChem 2950HP instrument (Micromeritics Instrument Corp., Norcross, GA, USA).

Before the experiments, catalysts were reduced in a hydrogen flow at 250 °C for 2 h. The FAMEs reactions were carried out in a stainless steel autoclave (15 ml) at temperature of 240 °C and H_2 pressure of 2.5 MPa for 2 h. The catalyst loading was 45 mg, substrate/Me molar ratio was 10. Dodecane was used as internal standard with the loading of 120 mg while ethanol was used as the solvent (V = 7 ml). The reaction products were analyzed on the Crystal-5000 GC-FID with the ZB-5 column (length 30 m, diameter 0.53 mm). The activity of the catalysts was evaluated by the FAMEs conversion.

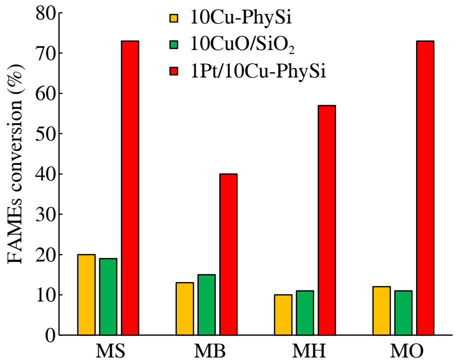

Figure 1 FAMEs conversion over copper-based catalysts at 240 °C and 2.5 MPa H_2.

synthesized catalysts were investigated in the liquid-phase selective hydrogenation reactions of methyl stearate (MS) to 1-octadecanol, methyl butyrate (MB) to 1-butanol, methyl hexanoate (MH) to 1-hexanol and methyl oleate (MO) to oleyl alcohol. The main products in these reactions were the corresponding alcohols; however, trace amounts of products of the side reaction of transesterification were detected. Figure 1 shows the conversion of FAMEs over monometallic copper catalysts. It can be seen that the activity of the copper phyllosilicate phase is almost identical to the catalytic activity of the copper oxide phase.

The modification of the monometallic 10Cu-PhySi catalyst by doping with noble metal (Pt) allowed us to enhance the activity of the catalyst (Figure 1). We have preliminary studied the effect of platinum addition on monometallic 10CuO/SiO$_2$ catalysts in the MH hydrogenation reaction, but the MH conversion was significantly lower than that of the catalyst comprising platinum deposited on the copper phyllosilicate phase. Consequently, we focused on the study of 1Pt/10Cu-PhySi catalyst. The addition of 1 wt% Pt increased the conversion of FAMEs several times compared with the monometallic copper samples. The conversion of the esters thus increased as follows: methyl stearate – from 20 to 73%, methyl butyrate – from 13 to 40%, methyl hexanoate – from 10 to 57% and methyl oleate – from 11 to 73%.

The phase composition of the synthesized catalysts was examined by XRD method. The formation of Cu phyllosilicate was observed on the XRD profile of 10Cu-PhySi catalyst (Figure 2), as evidenced by the presence of broadened reflexes at 34.5, 42.7 and 44.8°, which correlate with the reflexes of dioptase (PDF#33-487). XRD profile of 10CuO/SiO$_2$ catalyst showed the presence of crystallized CuO nanoparticles as attested by the existence of characteristic reflections at 36, 38, 49, 57, 63, 66 and 68°. The study of the phase composition of the bimetallic 1Pt/10Cu-PhySi catalyst showed the presence of reflexes at 35, 57 and 62°, which is consistent with the formation of Cu phyllosilicate phase. However, because of the small amount of platinum in the sample, which can not be detected by the XRD method, the reflex at 35° is likely to be attributed to the phyllosilicate phase.

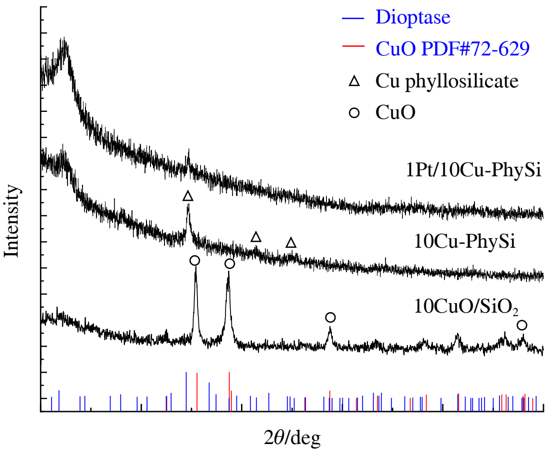

Figure 2 XRD profiles of mono- and bimetallic copper catalysts.

H_2-TPR method was used to investigate the reducibility of the calcined copper-based samples (Figure 3). Considering that a strong metal-support interaction may exist in 10Cu-PhySi catalyst, the reduction peak of the calcined 10CuO/SiO$_2$ sample shall occur at higher temperature. However, the H_2-TPR reveals that 10Cu-PhySi reduction takes place at a lower temperature than 10CuO/SiO$_2$, as shown in Figure 3(*a*). Similar results were obtained earlier.[21,22] The reduction of Cu phyllosilicate species proceeded in two steps: first the reduction of Cu phyllosilicate into Cu^+ occurring in the temperature range from 100 to 300 °C with a maximum at 207 °C and then the reduction of Cu^+ to Cu^0 occurring above 600 °C. Therefore, in this case, the reduction of Cu phyllosilicate was only to Cu^+ species. The hydrogen uptake by the 10Cu-PhySi catalyst was higher than those of 10CuO/SiO$_2$ and has totaled 0.717 mmol g^{-1}.

The reduction curve of calcined bimetallic 1Pt/10Cu-PhySi catalyst [Figure 3(*b*)] showed a broad high intensity peak in the temperature range from 100 to 400 °C with a maximum at 220 °C and a shoulder at 253 °C. The peak at 220 °C corresponds to the reduction of Cu^{2+} to Cu^+ ions: smaller nanoparticles are

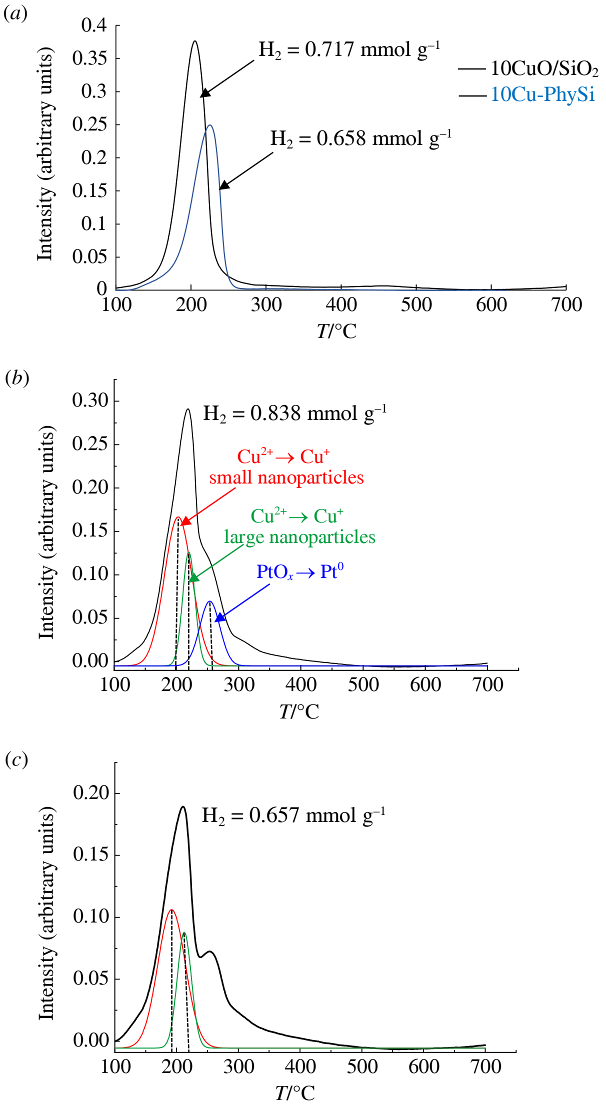

Figure 3 TPR-H_2 study of (*a*) calcined monometallic copper samples, (*b*) calcined 1Pt/10Cu-PhySi and (*c*) reduced 1Pt/10Cu-PhySi catalysts.

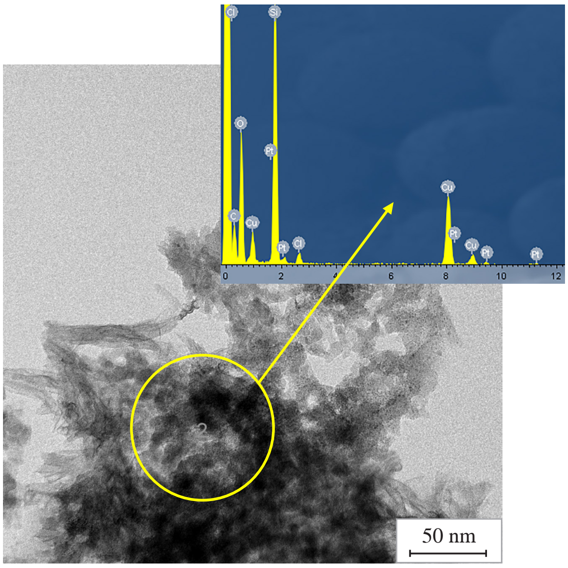

Figure 4 TEM image of the 1Pt/10Cu-PhySi catalyst.

reduced first (maximum at 200 °C), followed by larger nanoparticles (maximum at 220 °C). The reduction of PtO_x to Pt^0 is assumed to take place in one step at 253 °C. Comparison with the monometallic sample of copper phyllosilicate structure [Figure 3(*b*)] allows one to suggest that the Pt^0 phase in the bimetallic catalyst promotes easier reduction of copper phyllosilicate at lower temperatures.[23] The hydrogen uptake by the reduced 1Pt/10Cu-PhySi catalyst [Figure 3(*c*)] in this temperature range was substantially lower than those of calcined 1Pt/10Cu-PhySi, and totaled 0.657 mmol g^{-1}. This proves the partial reduction of Cu and full reduction of Pt in the sample when the sample is reduced at 250 °C before catalytic test.

The morphology of the bimetallic 1Pt/10Cu-PhySi catalyst was studied by TEM-EDX method (Figure 4). The microphotograph shows the ‘fibrous’ structure of the 10Cu-PhySi carrier that correlates with the structure of phyllosilicate. The formation of small spherical nanoparticles with an average diameter of ~1.2 nm was clearly observed. EDX analysis of this sample indicates the presence of Pt and Cu in the catalyst. Thus, based on the result of EDX analysis, the morphology corresponds to the formation of Pt particles on the copper phyllosilicate surface.

In conclusion, the addition of second metal resulted in the synergistic interaction with the copper phyllosilicate phase and an increase in the catalytic activity in the FAMEs hydrogenation. Thus, the best catalytic properties were demonstrated by the bimetallic 1Pt/10Cu-PhySi catalyst containing 1 wt% of Pt. Over 1Pt/10Cu-PhySi catalyst the FAMEs conversion of 40–73% was achieved at 240 °C and H_2 pressure of 2.5 MPa.

This study was supported by the Russian Science Foundation, grant no. 23-73-01034, https://rscf.ru/en/project/23-73-01034/.

References

1 J. Pitchard, A. Ciftci, M. W. G. M. (Tiny) Verhoeven, E. J. M. Hensen and E. A. Pidko, *Catal. Today*, 2017, **279**, 10; https://doi.org/10.1016/j.cattod.2016.03.043.

2 A. Corma, S. Iborra and A. Velty, *Chem. Rev.*, 2007, **107**, 2411; https://doi.org/10.1039/C5CS00038F.

3 J. Pitchard, G. A. Filonenko, R. van Putten, E. J. M. Hensen and E. A. Pidko, *Chem. Soc. Rev.*, 2015, **44**, 3808; https://doi.org/10.1039/C5CS00038F.

4 E. Menalla, J. G. Serna, D. Cantero and M. J. Cocero, *J. Chem. Eng.*, 2024, **493**, 152391; https://doi.org/10.1016/j.cej.2024.152391.

5 Z. Chen, H. Ge, P. Wang, J. Sun, M. Abbas and J. Chen, *Mol. Catal.*, 2020, **488**, 110919; https://doi.org/10.1016/j.mcat.2020.110919.

6 C. E. Berdugo-Díaz, M. T. Manetsch, J. Lee, Y. S. Yun, D. F. Yancey, S. J. Rozeveld, J. Luo, X. Chen and D. W. Flaherty, *J. Catal.*, 2024, **430**, 115346; https://doi.org/10.1016/j.jcat.2024.115346.

7 M. Eini and D. Tamarkin, *Patent US 6994863 B2*, 2006; https://patentimages.storage.googleapis.com/cf/76/32/9cc2861e8d61ab/US6994863.pdf.

8 Y. S. Yun, C. E. Berdugo-Díaz, J. Luo, D. G. Barton, I. Chen, J. Lee and D. W. Flaherty, *J. Catal.*, 2022, **411**, 212; https://doi.org/10.1016/j.jcat.2022.05.014.

9 A. T. Ubando, C. B. Felix and W.-H. Chen, *Bioresour. Technol.*, 2020, **299**, 122585; https://doi.org/10.1016/j.biortech.2019.122585.

10 Z. Rahmawati, J. A. Anderson and A. J. McCue, *Appl. Catal., A*, 2023, **666**, 119437; https://doi.org/10.1016/j.apcata.2023.119437.

11 A. M. Smith and R. Whyman, *Chem. Rev.*, 2014, **114**, 5477; https://doi.org/10.1021/cr400609m.

12 T. Miyake, T. Makino, S. Taniguchi, H. Watanuki, T. Niki, S. Shimizu, Y. Kojima and M. Sano, *Appl. Catal., A*, 2009, **364**, 108; https://doi.org/10.1016/j.apcata.2009.05.036.

13 X. Cao, S. Wu, J. Zhao, F. Long, S. Jia, X. Zhang, J. Xu and J. Jiang, *Appl. Catal., B*, 2024, **343**, 123506; https://doi.org/10.1016/j.apcatb.2023.123506.

14 Y. Yao, X. Wu, O. Y. Gutiérrez, J. Ji, P. Jin, S. Wang, Y. Xu, Y. Zhao, S. Wang, X. Ma and J. A. Lercher, *Appl. Catal., B*, 2020, **267**, 118698; https://doi.org/10.1016/j.apcatb.2020.118698.

15 R.-Ye, L. Lin, L.-C. Wang, D. Ding, Z. Zhou, P. Pan, Z. Xu, J. Liu, H. Adidharma, M. Radosz, M. Fan and Y.-G. Yao, *ACS Catal.*, 2020, **10**, 4465; https://doi.org/10.1021/acscatal.9b05477.

16 N. Sarki, S. Kumawat, M. Choudhary, A. Narani, S. K. Singh and K. Natte, *J. Catal.*, 2024, **429**, 115248; https://doi.org/10.1016/j.jcat.2023.115248.

17 X. Yu, T. A. Vest, N. Gleason-Boure, S. G. Karakalos, G. L. Tate and M. Burkholder, *J. Catal.*, 2019, **380**, 289; https://doi.org/10.1016/j.jcat.2019.10.001.

18 A. A. Shesterkina, K. V. Vikanova, V. S. Zhuravleva, A. L. Kustov, N. A. Davshan, I. V. Mishin, A. A. Strekalova and L. M. Kustov, *Mol. Catal.*, 2023, **547**, 113341; https://doi.org/10.1016/j.mcat.2023.113341.

19 W. Di, J. Cheng, S. Tian, J. Li, J. Chen and Q. Sun, *Appl. Catal., A*, 2016, **510**, 244; https://doi.org/10.1016/j.apcata.2015.10.026.

20 A. A. Shesterkina, V. S. Zhuravleva, K. E. Kartavova, A. A. Strekalova, K. V. Vikanova and A. L. Kustov, *Mendeleev Commun.*, 2024, **34**, 569; https://doi.org/10.1016/j.mencom.2024.06.033.

21 F. Li, L. Wang, X. Han, Y. Cao, P. He and H. Li, *Int. J. Hydrogen Energy*, 2017, **42**, 2144; https://doi.org/10.1016/j.ijhydene.2016.09.064.

22 Z.-Q. Wang, Z.-N. Xu, S.-Y. Peng, M. Zhang, G. Lu, Q.-S. Chen, Y. Chen and F.-K. Zheng, *ACS Catal.*, 2015, **5**, 4255; https://doi.org/10.1021/acscatal.5b00682.

23 B. Darif, S. Ojala, L. Pirault-Roy, M. Bensitel, R. Brahmi and R. L. Keiski, *Appl. Catal., B*, 2016, **181**, 24; https://doi.org/10.1016/j.apcatb.2015.07.050.

Received: 12th August 2024; Com. 24/7591